Investigation of negative-parity states in ^{156}Dy: Search for evidence of tetrahedral symmetry

D. J. Hartley *et al.*

Phys. Rev. C **95**, 014321 — Published 20 January 2017

DOI: 10.1103/PhysRevC.95.014321

Investigation of negative-parity states in ^{156}Dy: Search for evidence of tetrahedral symmetry

D. J. Hartley,[1] L. L. Riedinger,[2] R. V. F. Janssens,[3] S. N. T. Majola,[4] M. A. Riley,[5] J. M. Allmond,[6,7] C. W. Beausang,[6] M. P. Carpenter,[3] C. J. Chiara,[3,8,9,*] N. Cooper,[10] D. Curien,[11,12] B. J. P. Gall,[11,12] P. E. Garrett,[13] F. G. Kondev,[9] W. D. Kulp,[14] T. Lauritsen,[3] E. A. McCutchan,[3,15] D. Miller,[2,†] S. Miller,[5] J. Piot,[11,12] N. Redon,[16] J. F. Sharpey-Schafer,[17] J. Simpson,[18] I. Stefanescu,[3,8] X. Wang,[5,‡] V. Werner,[10,§] J. L. Wood,[14] C.-H. Yu,[7] S. Zhu,[3] and J. Dudek[11,19]

[1]*Department of Physics, U.S. Naval Academy, Annapolis, Maryland 21402, USA*
[2]*Department of Physics and Astronomy, University of Tennessee, Knoxville, Tennessee 37996, USA*
[3]*Physics Division, Argonne National Laboratory, Argonne, Illinois 60439, USA*
[4]*iThemba LABS, National Research Foundation, P.O. Box 722, Somerset-West 7129, South Africa*
[5]*Department of Physics, Florida State University, Tallahassee, Florida 32306, USA*
[6]*Department of Physics, University of Richmond, Richmond, Virginia 23173, USA*
[7]*Physics Division, Oak Ridge National Laboratory, Oak Ridge, Tennessee 37831, USA*
[8]*Department of Chemistry and Biochemistry, University of Maryland, College Park, Maryland 20742, USA*
[9]*Nuclear Engineering Division, Argonne National Laboratory, Argonne, Illinois, 60439, USA*
[10]*Wright Nuclear Structure Laboratory, Yale University, New Haven, Connecticut 06520, USA*
[11]*Université de Strasbourg, IPHC, 23 rue du Loess 67037 Strasbourg, France*
[12]*CNRS, UMR7178, 67037, Strasbourg, France*
[13]*Department of Physics, University of Guelph, Guelph, Ontario, N1G2W1 Canada*
[14]*School of Physics, Georgia Institute of Technology, Atlanta, Georgia 30332, USA*
[15]*National Nuclear Data Center, Brookhaven National Laboratory, Upton, New York 11973, USA*
[16]*Institut de Physique Nucléaire Lyon, IN2P3-CNRS, Lyon, F-69622 Villeurbanne, France*
[17]*Department of Physics, University of Western Cape, P/B X17, Bellville 7535, South Africa*
[18]*STFC Daresbury Laboratory, Daresbury, Warrington, WA4 4AD, United Kingdom*
[19]*Institute of Physics, University of Marie Curie-Sklodowska, Lublin, 20 031 Poland*

An experiment populating low/medium-spin states in ^{156}Dy was performed to investigate the possibility of tetrahedral symmetry in this nucleus. In particular, focus was placed on the low-spin, negative-parity states since recent theoretical studies suggest that these may be good candidates for this high-rank symmetry. The states were produced in the ^{148}Nd(^{12}C,4n) reaction and the Gammasphere array was utilized to detect the emitted γ rays. $B(E2)/B(E1)$ ratios of transition probabilities from the low-spin, negative-parity bands were determined and used to interpret whether these structures are best associated with tetrahedral symmetry or, as previously assigned, to octupole vibrations. In addition, several other negative-parity structures were observed to higher spin and two new sequences were established.

PACS numbers: 21.10.Re, 23.20.Lv, 27.70.+q

I. INTRODUCTION

Predictions of the possible presence of tetrahedral symmetry [1–4] at low spins and excitation energy in nuclear spectra have prompted several experimental studies [5–7] in the $Z \approx 64$ and $N \approx 90$ region. These nucleon numbers are considered to be magic with respect to this tetrahedral symmetry. A characteristic feature of this nuclear shape is that, in its pure form, there would be no quadrupole or dipole moments. Thus, early theoretical work suggested that negative-parity structures associated with this high-rank symmetry would be characterized by levels with rotational-like spacing, but vanishing $B(E2)$ rates at the lowest spins, due to the nucleus approaching the tetrahedral limit as it nears the bandhead [2]. Indeed, many negative-parity, odd-spin bands in even-even nuclei of the rare-earth region appear to satisfy this condition, including a sequence in ^{156}Dy. Therefore, a re-investigation of this nucleus utilizing the high resolving power of the Gammasphere array was warranted.

Within the past few years, the theoretical focus has moved away from a stable tetrahedral shape, to the possibility of tetrahedral "oscillations" about the ground-state quadrupole deformation [3]. These oscillations are analogous to the well-known γ vibrations with geometrical shapes described by the non-axial quadrupole Y_{22} spherical harmonic; the tetrahedral ones are then caused by the non-axial octupole $Y_{32} + Y_{3-2}$ spherical harmonic. However, identifying a firm experimental fingerprint of tetrahedral symmetry clearly distinguishing it from the more

*Present address: U.S. Army Research Laboratory, Adelphi, Maryland 20783, USA
†Present address: Idaho National Laboratory, Idaho Falls, Idaho 83402, USA
‡Present address: Department of Physics, California Polytechnic State University, San Luis Obispo, California 93407, USA
§Present address: Institut für Kernphysik, Technische Universität Darmstadt, 64289, Darmstadt, Germany

conventional interpretation in terms of an octupole (Y_{30}) vibration remains a challenge. In Refs. [3, 7], it has been suggested that tetrahedral vibrational bands would have negative parity with $K^\pi = 2^-$ and a transition strength ratio of the inband $E2$ over the interband $E1$ decays, $B(E2)/B(E1)$, an order of magnitude greater than for octupole vibrational bands. The current work focuses on interpreting the low-spin, negative-parity states in ^{156}Dy, as well as on extending the negative-parity, quasiparticle structures. It is worth noting that a study of the positive-parity levels in ^{156}Dy from the same experiment was recently published in Ref. [8].

II. EXPERIMENTAL DETAILS

Excited states of ^{156}Dy were populated via the ^{148}Nd(^{12}C,4n) reaction, where the ^{12}C beam was accelerated by the ATLAS facility at Argonne National Laboratory to an energy of 65 MeV. The target consisted of an isotopically-enriched (>99%) ^{148}Nd foil that was 1.5 mg/cm^2 thick, and was sandwiched between a 15.9 mg/cm^2 lead backing and a 0.1 mg/cm^2 flashing of gold to prevent oxidation. Gammasphere [9] was utilized to detect the γ-ray emissions, where 100 high-purity, germanium detectors were in operation. A beam intensity of ∼1.6 pnA was sustained throughout the three-day experiment.

In the off-line analysis, the data were sorted into a Blue [10] database, where approximately 2×10^9 3-fold (or greater) events were stored. A Radware [11] coincidence cube (E_γ-E_γ-E_γ) was created from this database in order to analyze the coincident spectra generated from the recorded events. A partial level scheme for ^{156}Dy is provided in Fig. 1, which focuses on the negative-parity structures that were extended, or observed for the first time, in this experiment. Note that the sequence associated with the $\nu(i_{13/2}, h_{11/2})$ configuration [12] is not shown in Fig. 1 as no new information was obtained.

In order to assist with spin assignments, a matrix was constructed where transitions detected in rings located at 70° to 100° were placed along one axis and the coincident transitions detected in forward rings at 31.7° to 51.1°, as well as backward angles 142.6° to 162.7°, along the other axis (F/B). Directional correlation of oriented states (DCO) ratios were then determined by placing coincidence gates on both axes using a known stretched electric quadrupole ($E2$) transition, and then comparing the intensities of the coincident γ rays by $R_{DCO} = I_\gamma(\theta = F/B)/I_\gamma(\theta \approx 90°)$. Ratios of $R_{DCO} \approx 1$ are expected for stretched-$E2$ transitions, and $R_{DCO} \approx 0.6$ for pure electric and magnetic dipole ($E1$ and $M1$, respectively) transitions. The energies of the levels, as well as the energies, relative intensities, and DCO ratios of the γ rays involved are provided in Table I.

TABLE I: Gamma-ray energies and intensities in ^{156}Dy.

$I^{\pi\,a}$	E_{level} (keV)	E_γ (keV)^b	$I_\gamma{}^c$	R_{DCO}	Band$_f$, I$_f^{\pi\,d}$
		Band 1			
0^+	0.0				
2^+	137.7	137.7	∼61^e	0.86(1)	1, 0^+
4^+	404.1	266.4	≡100	0.99(1)	1, 2^+
6^+	770.3	366.2	97(6)	0.94(1)	1, 4^+
8^+	1215.6	445.3	81(5)	0.95(1)	1, 6^+
10^+	1724.8	509.2	58(4)	0.91(1)	1, 8^+
12^+	2285.7	560.9	39(2)	0.94(1)	1, 10^+
14^+	2887.7	602.0	29(2)	0.88(1)	1, 12^+
16^+	3523.2	635.5	11.4(7)		1, 14^+
18^+	4178.4	655.2	7.1(4)		1, 16^+
20^+	4859.2	680.8	3.4(2)		1, 18^+
22^+	5573.1	713.9	1.7(1)		1, 20^+
24^+	6329.0	755.9	0.48(5)		1, 22^+
26^+	7130.4	801.4	0.15(2)		1, 24^+
28^+	7978.3	847.9	0.06(2)		1, 26^+
		Band 2			
5^-	1525.5	1121.4	0.39(2)	0.83(2)^f	1, 4^+
		755.0	0.13(1)	0.67(1)^f	1, 6^+
7^-	1809.8	1039.5	1.21(7)	0.63(1)	1, 6^+
		594.1	0.08(1)		1, 8^+
9^-	2186.1	376.3	0.04(1)		2, 7^-
		970.5	2.3(1)	0.54(1)	1, 8^+
11^-	2636.4	449.4	0.37(2)		2, 9^-
		911.6	2.7(1)	0.57(1)	1, 10^+
13^-	3154.2	517.9	0.72(4)		2, 11^-
		868.5	1.45(9)		1, 12^+
15^-	3719.8	565.6	1.25(8)		2, 13^-
		832.1	1.08(9)		1, 14^+
17^-	4331.1	611.3	1.46(9)		2, 15^-
		807.9	0.55(4)		1, 16^+
19^-	4978.0	646.9	0.70(4)		2, 17^-
		(800)	< 0.01		1, 18^+
21^-	5658.5	680.5	0.48(3)		2, 19^-
23^-	6374.7	716.2	0.28(2)		2, 21^-
25^-	7129.4	754.7	0.15(1)		2, 23^-
27^-	7925.9	796.5	0.06(1)		2, 25^-
		Band 3			
9^-	2610.6	1394.8	0.39(2)	0.55(3)	1, 8^+
		885.8	0.05(1)		1, 10^+
		752.0	0.06(1)		SV, 8^+
11^-	3040.5	429.9	0.32(2)		3, 9^-
		1315.7	0.08(1)		1, 10^+
		854.2	0.19(1)		2, 9^-
		724.9	0.17(1)		SV, 10^+
		404.2	0.27(2)		2, 11^-
13^-	3515.3	474.8	0.30(2)		3, 11^-
		879.0	0.11(1)		2, 11^-
		477.6	0.10(1)		8, 11^-
		361.2	0.11(1)		2, 13^-
15^-	4060.1	544.8	0.30(2)		3, 13^-
		340.3	0.07(1)		2, 15^-
17^-	4646.4	586.3	0.21(1)		3, 15^-
19^-	5228.8	582.4	0.13(1)		3, 17^-
		(548)	< 0.01		3a, 17^-
		Band 3a			
(17^-)	4681.3	621.2	0.02(1)		3, 15^-
(19^-)	5315.4	634.1	0.01(1)		3a, 17^-
		(669)	< 0.01		3, 17^-
		Band 4			

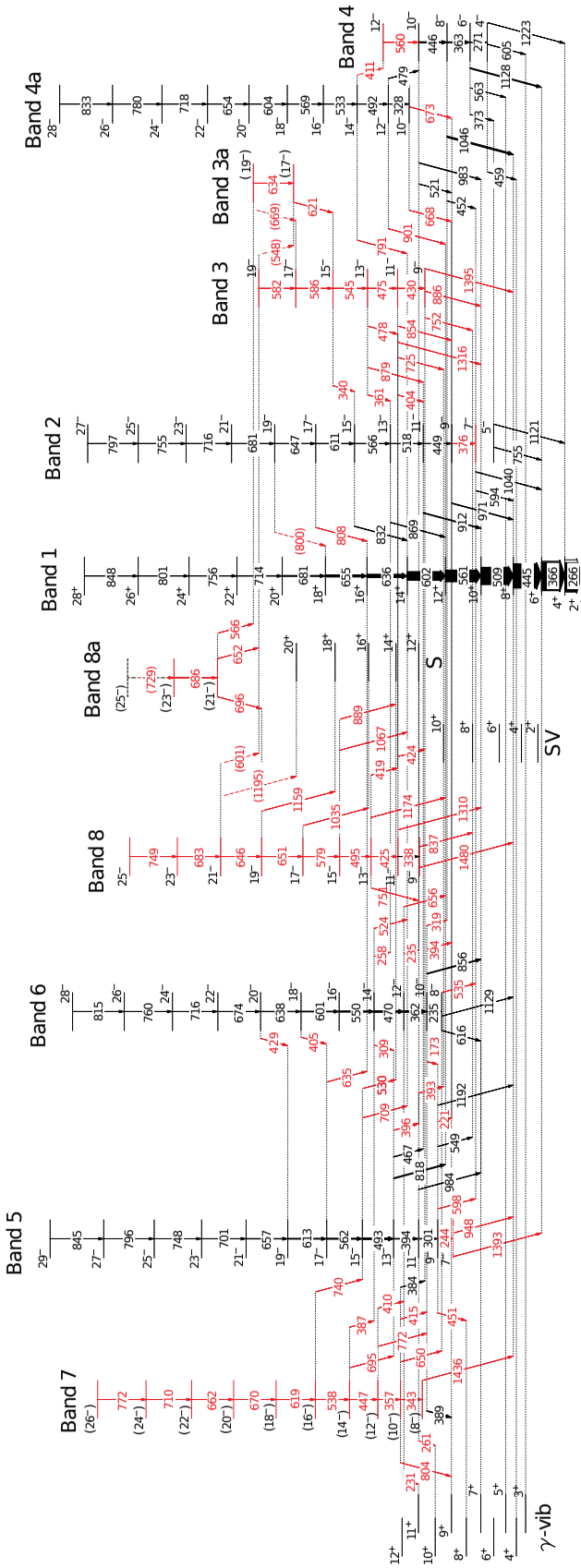

FIG. 1: (Color online) Partial level scheme for ^{156}Dy from the present analysis emphasizing the new negative-parity states. Tentative levels and γ rays are given as dashed lines and new transitions are shown in red. Note that the strongly-coupled, negative-parity structure in Ref. [12] is not shown and many of these sequences were extended to higher spin in Ref. [13].

4^-	1627.0	1222.9	0.28(2)	0.85(7)	1, 4^+			535.3	0.03(1)		2, 7^-
		605.0	0.10(7)		γ-vib, 3^+	10^-	2580.3	235.1	0.82(6)	0.94(1)	6, 8^-
		459.0	0.01(1)		γ-vib, 4^+			855.5	2.9(2)	0.93(1)	1, 10^+
6^-	1898.1	271.1	0.37(2)		4, 4^-			394.1	0.20(3)		2, 9^-
		1127.8	3.4(2)	0.94(2)	1, 6^+			389.0	2.1(2)	0.67(1)	γ-vib, 9^+
		562.6	0.19(1)		γ-vib, 5^+			319.0	0.39(3)	1.02(2)	4, 8^-
		372.6	0.40(2)		2, 5^-			172.6	0.17(2)	0.41(1)	5, 9^-
8^-	2261.2	363.1	3.2(2)	1.00(1)	4, 6^-	12^-	2942.0	361.7	5.7(3)		6, 10^-
		1045.7	5.2(3)	0.92(1)	1, 8^+			656.3	0.71(4)		1, 12^+
		451.6	0.70(4)		2, 7^-			234.5	0.31(2)		4, 10^-
10^-	2707.5	446.3	3.8(7)		4, 8^-			230.5	0.23(2)		γ-vib, 11^+
		982.9	1.9(1)	0.96(1)	1, 10^+	14^-	3411.8	469.8	5.0(4)	1.04(1)	6, 12^-
		521.3	0.59(4)		2, 9^-			524.2	0.08(1)		1, 14^+
12^-	3267.0	559.5	0.21(3)		4, 10^-			308.7	0.25(2)		5, 13^-
		Band 4a						257.7	0.14(1)		2, 13^-
10^-	2858.8	672.6	0.04(1)		2, 9^-	16^-	3961.9	550.1	4.2(2)	1.00(1)	6, 14^-
		667.7	0.07(1)		γ-vib, 9^+	18^-	4562.8	600.9	2.6(2)	0.82(1)	6, 16^-
12^-	3186.6	327.8	0.05(1)		4a, 10^-			404.6	0.10(1)		5, 17^-
		901.2	0.27(2)		1, 12^+	20^-	5200.4	637.6	1.30(8)	0.86(1)	6, 18^-
		479.1	1.47(8)	0.96(1)	4, 10^-			429.1	0.06(1)		5, 19^-
		485.7	0.48(3)		AY,[g] 10^-	22^-	5873.9	673.5	0.67(4)		6, 20^-
14^-	3678.1	491.5	1.50(8)	0.92(1)	4a, 12^-	24^-	6589.8	715.9	0.28(2)		6, 22^-
		790.7	0.06(1)		1, 14^+	26^-	7349.7	759.9	0.05(1)		6, 24^-
		410.9	0.07(1)		4, 12^-	28^-	8164.6	814.9	0.06(1)		6, 26^-
16^-	4210.8	532.7	1.19(7)		4a, 14^-			Band 7			
18^-	4779.5	568.7	0.89(6)		4a, 16^-	(8^-)	2651.5	1435.9	0.04(1)		1, 8^+
20^-	5383.0	603.5	0.74(4)		4a, 18^-	(10^-)	2994.8	343.3	0.03(1)		7, 8^-
22^-	6037.2	654.2	0.39(2)		4a, 20^-			803.7	0.05(1)		γ-vib, 9^+
24^-	6754.9	717.7	0.21(2)		4a, 22^-			649.8	0.05(1)		6, 8^-
26^-	7534.8	779.9	0.11(1)		4a, 24^-			414.7	0.15(1)		6, 10^-
28^-	8367.7	832.9	0.10(1)		4a, 26^-			384.2	0.01(1)		3, 9^-
		Band 5				(12^-)	3351.8	357.0	0.29(1)		7, 10^-
7^-	2163.3	1393.0	0.13(1)		1, 6^+			771.7	0.06(1)		6, 10^-
		947.8	0.03(1)	0.67(3)	1, 8^+			409.8	0.24(1)		6, 12^-
9^-	2407.5	244.2	0.07(1)		5, 7^-	(14^-)	3798.4	446.6	0.31(5)		7, 12^-
		1191.9	0.61(4)	0.64(3)	1, 8^+			695.2	0.09(1)		5, 13^-
		597.7	0.03(1)		2, 7^-			386.7	0.09(1)		6, 14^-
		549.4	0.83(6)		SV, 8^+	(16^-)	4336.1	537.7	0.36(2)		7, 14^-
		450.7	0.42(3)		γ-vib, 8^+			739.8	0.04(1)		5, 15^-
		221.3	0.03(1)		2, 9^-	(18^-)	4955.4	619.3	0.39(2)		7, 16^-
11^-	2708.7	301.2	1.9(1)	0.97(1)	5, 9^-	(20^-)	5625.3	669.9	0.12(1)		7, 18^-
		984.1	1.56(8)	0.73(2)	1, 10^+	(22^-)	6287.7	662.4	0.06(1)		7, 20^-
		393.1	1.3(2)		SV, 10^+	(24^-)	6997.3	709.6	0.03(1)		7, 22^-
		261.3	0.26(2)		γ-vib, 10^+	(26^-)	7769.4	772.1	0.01(1)		7, 24^-
13^-	3103.1	394.4	2.0(2)	0.97(1)	5, 11^-			Band 8			
		817.8	3.4(2)	0.58(1)	1, 12^+	9^-	2696.0	1480.4	0.08(1)		1, 8^+
		467.3	1.32(7)		2, 11^-			837.4	0.03(1)		SV, 8^+
		396.4	0.52(3)		S, 12^+	11^-	3034.4	338.4	0.05(1)		8, 9^-
15^-	3595.9	492.8	5.3(3)		5, 13^-			1309.8	0.47(3)	0.53(3)	1, 10^+
		708.6	0.68(4)		1, 14^+			423.9	0.08(2)		3, 9^-
		529.8	0.06(1)		S, 14^+	13^-	3459.1	424.7	0.44(4)		8, 11^-
17^-	4157.8	561.9	3.6(2)		5, 15^-			1173.7	0.29(2)		1, 12^+
		634.9	0.27(2)		1, 16^+			750.5	0.09(1)		5, 11^-
19^-	4771.2	613.4	2.9(2)		5, 17^-			418.8	0.12(1)		3, 11^-
21^-	5428.5	657.3	1.50(9)		5, 19^-	15^-	3954.4	495.3	0.52(3)		8, 13^-
23^-	6129.7	701.2	0.70(4)		5, 21^-			1066.7	0.03(1)		1, 14^+
25^-	6877.2	747.5	0.26(2)		5, 23^-			888.7	0.08(1)		S, 14^+
27^-	7673.0	795.8	0.12(1)		5, 25^-	17^-	4533.4	579.0	0.65(4)		8, 15^-
29^-	8518.0	845.0	0.03(1)		5, 27^-			1034.8	0.15(1)		S, 16^+
		Band 6				19^-	5184.2	650.8	0.41(2)		8, 17^-
8^-	2345.2	1129.4	0.16(1)	0.96(1)	1, 8^+			1158.6	0.06(1)		S, 18^+
		616.4	1.00(6)	0.77(1)	γ-vib, 7^+	21^-	5830.0	645.8	0.10(1)		8, 19^-

		(1195)	< 0.01	S, 20^+
		(601)	< 0.01	3, 19^-
23^-	6513.3	683.3	0.06(1)	8, 21^-
25^-	7262.7	749.4	0.03(1)	8, 23^-
		Band 8a		
(21^-)	5880.5	696.3	0.06(1)	8, 19^-
		651.8	0.06(1)	3, 19^-
		566.0	0.05(1)	3a, 19^-
(23^-)	6566.0	685.5	0.03(1)	8a, 21^-
(25^-)	(7295)	(729)	0,01(1)	8a, 23^-

[a] Spin and parity of the depopulated state.
[b] Uncertainties in γ-ray energy are 0.2 keV for most transitions, except for relatively weak ones ($I_\gamma < 1$) where 0.5 keV uncertainties are assigned.
[c] Relative intensity of the transition with respect to that of the 266.4-keV transition.
[d] Band and state fed by the γ ray.
[e] Estimated based on intensity balance considerations.
[f] Unresolved doublet.
[g] Transition feeds state in structure assigned as the $\nu(i_{13/2}, h_{11/2})$ configuration in Ref. [12] and is not displayed in Fig. 1.

III. LEVEL SCHEME

A. Band 1

The sequence labeled as band 1 in Fig. 1 is the ground-state band of ^{156}Dy. Although this structure was only observed up to spin $I = 28$ in this experiment, it has been delineated up to $I = (58^+)$ by Kondev *et al.* [13]. This band is displayed since the negative-parity structures feed it. Feeding by negative-parity levels also justifies the presence in Fig. 1 of the positive-parity, second vacuum sequence [8] (labeled as SV), the S band (labeled S), and the γ-vibrational band (labeled as γ-vib).

B. Bands 2, 3, 4, and 4a

Band 2 is the structure of primary interest for this investigation in regard to it possibly displaying characteristics of tetrahedral symmetry [1]. This issue will be addressed in Sec. IV.B along with arguments to associate bands 2-4a with each other. Band 2 was previously observed up to $I^\pi = 19^-$ [12], but is now extended to 27^-. A double coincidence gate placed on the 611-keV inband and 832-keV linking transitions produced the spectrum displayed in Fig. 2(a), which illustrates how the sequence was extended. Note the strong presence of the ground-state band transitions below the 14^+ state, where the 832-keV line feeds. The 376-keV transition between the 9^- and 7^- states in band 2 was observed for the first time; however, the 284-keV line that should connect the 7^- to the 5^- level was below the detection limit of this experiment. Indeed, the inband $E2$ transitions become quite weak as spin decreases (see in Table I), a point to be addressed in Sec. IV. In addition, two new linking

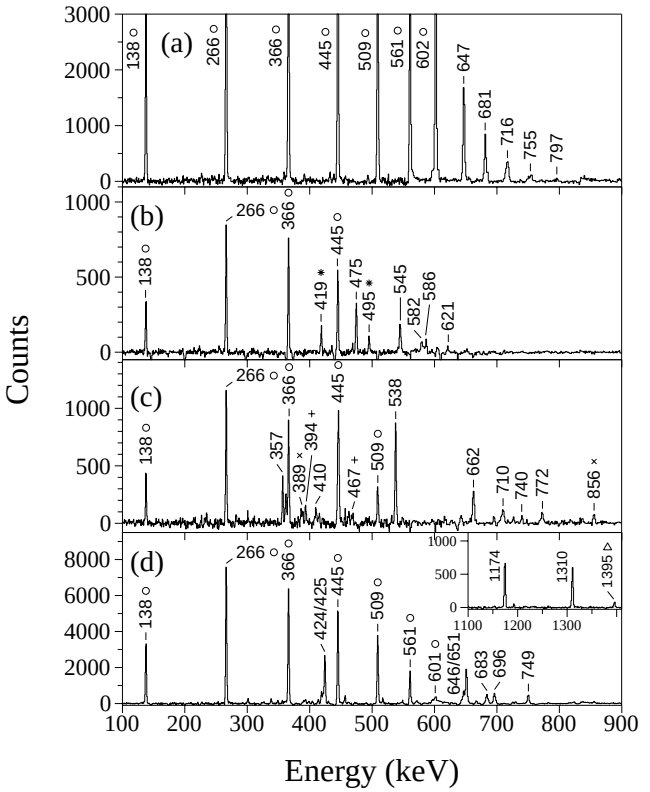

FIG. 2: (a) Representative spectrum for band 2 created by taking a double gate in the coincidence cube on the 611- and 832-keV transitions. Transitions in this, and all panels, marked with a circle are associated with the ground-state sequence in ^{156}Dy. (b) Spectrum displaying γ rays associated with band 3. The double gate with the 430- and 1395-keV lines produced this spectrum. The γ rays marked with stars result from bands 3 and 8 being in coincidence. (c) Spectrum of transitions belonging to band 7 obtained by double gating with the 619- and 670-keV lines. Peaks denoted with a plus or cross result from coincidence relationships of band 7 with bands 5 and 6, respectively. (d) Representative spectrum for band 8 produced with a double gate on the 495- and 579-keV transitions; a high-energy insert is provided in the upper-right portion of the panel demonstrating the coincidence with the 1395-keV line from band 3.

transitions (808 and 800 keV) were placed between bands 2 and 1. The DCO ratios for the 755-, 1040-, 971-, and 912-keV linking transitions are consistent with all being pure dipole transitions, and this result coincides with the assignment of negative parity by de Boer *et al.* [14].

A sequence of transitions, labeled as band 3 in Fig. 1, feeds the ground-state and SV bands at lower spin, and then primarily decays to band 2 at higher spins. A representative spectrum is given in Fig. 2(b), where a double gate placed on the 430-keV inband and 1395-keV linking transitions displays the inband γ rays above the 11^- state. In addition, transitions feeding into band 3 can be observed in the spectrum and are drawn as band 3a in Fig. 1. Although many linking transitions are found decaying from band 3, only the 1395-keV line was strong

enough to confidently determine a DCO ratio. The value of 0.55(3) is consistent with a pure dipole character, which is likely to be $E1$ in nature. If the assumption of $M1$ was made for the 1395-keV γ ray, the 854-, 879-, and 340-keV lines would have $M2$ character, which is highly unlikely in prompt spectroscopy.

The majority of the levels associated with bands 4 and 4a have been previously observed. However, the spin/parity assignments for these states had never been confidently assigned. The lowest observed state at 1627 keV had been assumed to have $I^\pi = 4^+$ since it feeds three different positive-parity levels. Caprio *et al.* [15] recently identified a 271-keV transition from the 1898-keV level feeding into the 1627-keV state, where the former had previously been assigned 6^-. In the present data, we confirm the presence of the 271-keV line linking these states, and interpret it as an inband transition in band 4. This requires a negative-parity assignment for the 1627-keV state. The DCO ratio of the 1223-keV line from the 1627-keV level to the 4^+ member of the ground-state sequence is consistent with either a stretched-$E2$, or unstretched dipole γ ray, which could be either electric or magnetic. In addition, a recent DCO/polarization measurement confirms that the 1223-keV transitions has an $E1$, $I \rightarrow I$ nature [16]. Note that similar transitions exist from the higher states in band 4 (1128, 1046, and 983 keV: all feeding the ground-state sequence) with similar DCO ratios of approximately 1.0. If all of these states were of positive parity, one would expect to observe the stretched-$E2$ ($I \rightarrow I-2$) transitions, in addition to the $I \rightarrow I$ γ rays. The fact that these stretched-$E2$ lines are not seen may indicate that the high-energy transitions are unstretched $E1$ γ rays, and, thus, band 4 is assigned negative parity. In addition, transitions linking bands 4 and 2 are observed higher in the band, which also point toward a negative-parity assignment.

Band 4a has previously been observed [12] and a further study [17] concluded that the states involved have negative parity. This was included in the evaluation of Ref. [18]. Indeed, Refs. [17, 18] considered bands 4 and 4a as a single sequence and, as discussed below, this work agrees with the assignment proposed in Ref. [18]; however, the 12^- and 10^- states in bands 4 and 4a, respectively, were newly observed in the present study. Therefore, the two structures are drawn separately in Fig. 1. In addition, the 668-, 673-, 791-, and 901-keV linking transitions were observed for the first time.

C. Bands 5 and 6

The structures labeled as bands 5 and 6 in Fig. 1 have been previously observed to high spin [12, 13]. However, many new linking transitions from these sequences have been identified, including those feeding band 2. From band 5, the new transitions are: 948, 244, 598, 451, 221, 393, 261, 396, 709, 530, and 635 keV. The following transitions are newly assigned to decay from band 6: 535, 394, 319, 173, 656, 235, 231, 309, 258, 405, and 429 keV.

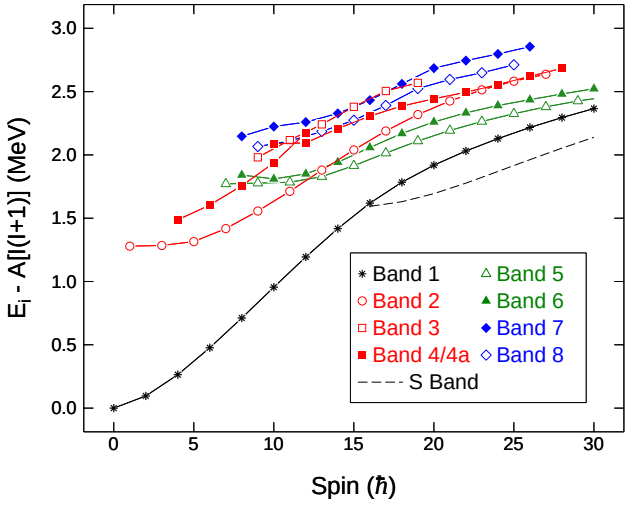

FIG. 3: (Color online) Energies of states (minus a rigid-rotor reference) versus spin for the bands displayed in Fig. 1. The moment of inertia parameter was chosen to be $A = 0.007$ MeV/$\hbar^2$. In addition to the structures displayed in Fig. 1, the S band is also given as it defines the yrast sequence at higher spins.

D. Bands 7 and 8

The new sequences labeled bands 7 and 8 exhibit several transitions feeding into the negative-parity bands 3, 5 and 6 in addition to the yrast positive-parity structures. Spectra for these bands are provided in Figs. 2(c) and (d), respectively. The interactions with the known negative-parity bands imply negative parity for bands 7 and 8. Only the 1310-keV line (from the 11^- state in band 8) was sufficiently strong to perform a DCO analysis. Its ratio was determined to be 0.53(3), which is consistent with a pure dipole transition. This 11^- state is also nearly degenerate with the 11^- level in band 3 ($\sim$6 keV separates the two), and cross-over transitions are observed between the bands (note the 424- and 419-keV γ rays from band 8 to band 3, and the 478-keV transition from band 3 to band 8). This interaction strongly indicates that the two levels must have the same spin and parity values, and allows for the spin/parity assignments proposed for band 8 in Fig. 1.

The spin/parity assignment for band 7 is more difficult; however, arguments for the values assigned can be made by examining the multiple decays out of the state at 2995 keV, which has been assigned as $I^\pi = 10^-$. This level feeds the known 8^- (band 6), 9^- (band 3), 9^+ (γ-vib), and 10^- (band 6) states. As stated above, band 7 very likely has negative parity; therefore, with the observed decays from this level, 8^-, 9^-, and 10^- assignments are possible for the 2995-keV state. The 8^- value can be eliminated as this would require a 6^- assignment for the

state at 2652 keV in band 7. This lower level feeds the 8^+ state of band 1 through the 1436-keV line and a 6^- assignment would require an $M2$ character for the 1436-keV γ ray, which is unlikely in prompt spectroscopy. To distinguish between the 9^- and 10^- assignments, it should be noted that the measured intensities of bands 3 and 7 are similar (see Table I) and, as seen in the rigid-rotor plot of Fig. 3, if one assigns the 2995-keV level as 10^-, the bands are close in energy which is consistent with their observed intensities. On the other hand, if the 9^- assignment is chosen, band 7 would be significantly higher in energy in Fig. 3 and one would expect lower intensities for this sequence compared to that in band 3. Therefore, the 10^- quantum numbers are preferred for the 2995-keV level, but must be regarded as tentative at this time.

IV. DISCUSSION

A. Configuration for Bands 7 and 8

The configurations of band 1 (ground-state band) and bands 5 and 6 [$\nu(i_{13/2}, h_{9/2})$] were previously assigned by Riley *et al.* [12], while the nature of bands 2-4 are addressed in the subsection below. At present, the quasiparticles responsible for bands 7 and 8 are discussed. Figure 4(a), which displays the aligned angular momentum (*i.e.*, alignment) for bands 1, 5, 6, 7, and 8 in ^{156}Dy, will aid in the configuration assignment of the latter sequences. Note that Harris parameters [19] of $\mathcal{J}_0 = 23$ $\hbar^2$/MeV and $\mathcal{J}_1 = 90$ $\hbar^4$/MeV^3 were used to subtract the angular momentum of the collective core.

The large initial alignment of bands 7 and 8 [>6 $\hbar$, see Fig. 4(a)] rules out a two-quasiproton assignment for these sequences as the quasiproton orbitals near the Fermi surface do not possess sufficiently large alignment values to reach 6 $\hbar$. In addition, as seen in Fig. 4(a), bands 7 and 8 track each other closely over nearly the full frequency range where they are observed. This is a strong indication that the two are signature partners of the same configuration. The large initial alignment suggests that an $i_{13/2}$ quasineutron is involved in the configuration and that it is likely paired with a negative-parity quasineutron to produce the negative-parity states.

It should also be noted that bands 7 and 8 as well as 5 and 6 track each other over the observed frequency range in Fig. 4(a). In addition, the energy splitting observed between band 7 and 8 in Fig. 3 is nearly identical to that seen between bands 5 and 6. Therefore, the configuration of bands 7 and 8 is likely correlated with that of bands 5 and 6. The possibility of bands 7 and 8 being based on the coupling of a γ-vibration phonon with bands 5 and 6 was considered. However, the energy associated with the γ vibration ($\sim$300 keV) in this scenario is much less than that of the γ-vibration band ($\sim$900 keV) known at low spin in ^{156}Dy. Thus, this interpretation is not likely to be valid. Another possibility is the $\nu(i_{13/2}, f_{7/2})$ configuration; however, such an assignment would change the energetically favored signature from $\alpha = 1$ in bands 5 and 6 to $\alpha = 0$ in bands 7 and 8. In contrast, as seen in Fig. 3, the two sets both display the odd-spin sequence lying lower in energy compared with the even-spin one. Thus, the proposed configuration for bands 7 and 8 is the identical $\nu(i_{13/2}, h_{9/2})$ assignment as for bands 5 and 6, but with the opposite (and energetically unfavored) K-coupling of the two quasineutrons.

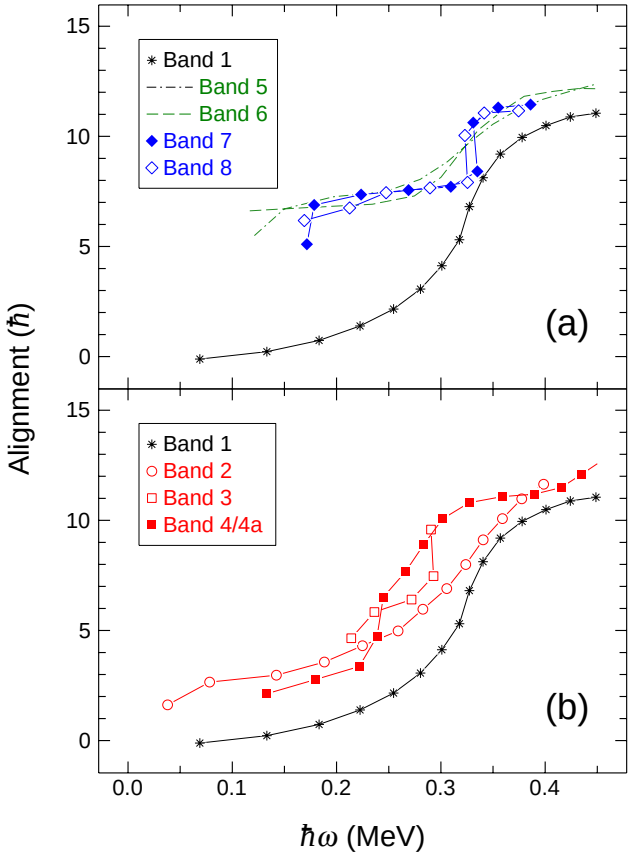

FIG. 4: (Color online) Alignment versus rotational frequency of (a) bands 1, 5, 6, 7, and 8, as well as (b) bands 1, 2, 3, 4, and 4a in ^{156}Dy.

B. Bands 2-4: Octupole Vibrations or Tetrahedral Symmetry?

The primary focus of this experiment was the nature of the lowest-lying negative-parity sequence, labeled as band 2 in Fig. 1. Previous works on ^{156}Dy assigned this structure as an octupole (Y_{30}) vibrational band [14]; however, as stated above, the possibility of tetrahedral ($Y_{32} + Y_{3-2}$) symmetry in the region near ^{156}Dy provided the motivation to revisit the character of this band with Gammasphere. As this discussion focuses on two possible types of octupole vibration, we refer the reader to the comprehensive works of Neergård and Vogel [20], as well as Butler and Nazarewicz [21], concerning this excitation mode.

Within the framework of group theory, Dudek *et al.* [1] proposed that structures resulting from tetrahedral symmetry could be observed at relatively low energies in nuclei with specific proton and neutron values. In particular, nuclei with proton numbers 64 or 70, and neutron number 90 were predicted to be "doubly magic" with respect to tetrahedral symmetry. It was suggested [2] that nuclei displaying effects from this high-rank symmetry would produce a collective structure of negative-parity levels, but that the quadrupole moment, and thus the in-band $B(E2)$ transition rate, would approach zero in the extreme limit. This limit would be most closely reached at the lowest spins in the band. Therefore, a set of rotational levels with "missing" $E2$ transitions at low spin may possibly be viewed as an indication for tetrahedral symmetry.

The $N = 90$ nucleus ^{156}Dy appears to have such a band, as strong $E1$ transitions connect band 2 to the ground-state sequence, but the in-band $E2$ transitions decrease in intensity until they can no longer be observed (below $I^\pi = 7^-$). In Ref. [12], the lowest $E2$ transition was found to depopulate the 11^- level while, in the present work, the lowest $E2$ inband transition is now seen from the 9^- state. In addition to the states shown in Fig. 1 for band 2, two other states have also been associated with this sequence: a 3^- level at 1368.4 keV and a 1^- one at 1293.4 keV [18]. Again, the $E2$ transitions are not observed between these levels, but strong $E1$ γ rays are found feeding the ground-state band.

In order to test whether the $B(E2)$ transition rate might be decreasing as spin decreases, the $B(E2)/B(E1)$ probability ratios for band 2 were determined by measuring the branching ratio λ between transitions from a state with spin I and using the relation

$$\frac{B(E2: I \rightarrow I-2)}{B(E1: I \rightarrow I-1)} = \frac{\lambda}{0.767}\frac{E_\gamma^3(I \rightarrow I-1)}{E_\gamma^5(I \rightarrow I-2)}(10^6 fm^2)$$

where E_γ is given in MeV. These ratios are given in Table II, together with those obtained for bands 4 and 4a. There is a clear decrease in the ratios as spin is reduced for band 2, and this observation could possibly indicate a decrease in the $B(E2)$ rate with spin.

Although this trend in the $B(E2)/B(E1)$ ratio is consistent with the tetrahedral theory, it is not sufficient to imply that this symmetry should be associated with band 2. Indeed, the trend can originate from two possible effects: (1) a $B(E2)$ rate decreasing with decreasing spin, which could be the result of tetrahedral symmetry, or (2) a $B(E1)$ rate increasing due to the octupole correlations associated with the Y_{30} spherical harmonic.

Lifetimes were recently measured for the lowest negative-parity band in ^{156}Gd [5], which also exhibits missing $E2$ transitions, making it another candidate for tetrahedral symmetry. The quadrupole moments of several of the negative-parity states of interest could be deduced. In addition, band mixing calculations allowing for an estimate of quadrupole moments were performed

TABLE II: Branching and $B(E2)/B(E1)$ ratios for bands 2, 4, and 4a in ^{156}Dy. When possible, the branching ratios, λ, were determined from spectra that resulted from coincidence gates placed directly above the state of interest.

I^π	$E_\gamma(E2)$ (keV)	$E_\gamma(E1)$ (keV)	λ	$B(E2)/B(E1)$ ($\times 10^6$ fm^2)
		Band 2		
9^-	376.3	970.5	0.020(4)	3.16(63)
11^-	449.4	911.6	0.144(7)	7.75(38)
13^-	517.9	868.5	0.43(3)	9.86(69)
15^-	565.6	832.1	1.36(8)	17.7(10)
17^-	611.3	807.9	2.8(2)	22.6(16)
		Band 4		
6^-	271.1	1127.8	0.121(8)	154(10)
8^-	363.1	1045.7	0.639(8)	151(2)
		Band 4a		
12^-	479.1	901.2	5.58(22)	211(8)
14^-	491.5	790.7	20.5(10)	460(22)

for the lowest negative-parity bands in the "tetrahedral doubly-magic" ^{154}Gd and ^{160}Yb [6] nuclei. In each of these cases, the quadrupole moments of the low-spin, negative-parity sequence were determined to be consistent with those measured in the ground-state bands of the respective nuclei. This is in contradiction with the original tetrahedral hypothesis of Ref. [2].

More recent theoretical investigations [3] indicate that the presence of a non-negligible quadrupole moment can be generated by the quadrupole vibrations around the equilibrium of pure tetrahedral symmetry, or perhaps as the result of "symmetry coexistence". The physics of coexisting symmetries is interesting, but further detailed discussion of this topic is outside the scope of the present work.

The question facing nuclear structure physicists regarding tetrahedral symmetry is whether an experimental fingerprint can be defined in order to contrast it with the more commonly accepted current interpretation in terms of an octupole vibration. Indeed, following their theoretical work on this topic, Zberecki *et al.* [22] described the prospects for experimentally confirming the existence of tetrahedral symmetry to be "problematic" due to the mixing of octupole and quadrupole deformations at higher spins.

Attention has turned away from the lowest, odd-spin, negative-parity band to the lowest, even-spin, negative-parity sequence. It has been noted [4] that the $B(E2)/B(E1)$ ratios for the even-spin bands are greatly different from those of the odd-spin ones. Indeed, this can be seen in Table II for ^{156}Dy as well as in Fig. 3 of Ref. [6] for ^{154,156}Gd and ^{160}Yb. Differences in these ratios are a factor of 10-100 between the odd- and even-spin negative-parity bands. Therefore, the question has been raised as to whether these bands can be interpreted as "partner"

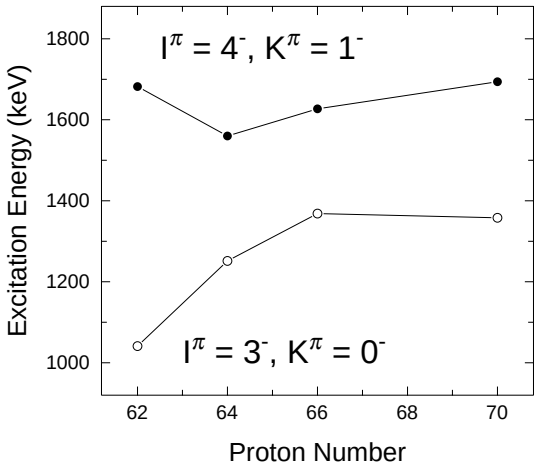

FIG. 5: Excitation energies of the 3^- state from the $K^\pi = 0^-$ octupole vibrational sequence and the 4^- state from the $K^\pi = 1^-$ octupole structure in the $N = 90$ isotones.

bands with such large disparities in the $B(E2)/B(E1)$ ratios.

However, as noted in Refs. [6, 23–25], these bands are likely octupole vibrations based on different K values, where the odd-spin sequence is assigned the $K = 0$ principal quantum number and the even-spin one for ^{152}Sm and ^{154}Gd has been assigned $K = 1$. Indeed, both the odd- and even-spin sequences of the $K^\pi = 1^-$ structure are observed in ^{152}Sm [24] and ^{154}Gd [25] in addition to the decoupled $K^\pi = 0^-$ band.

Figure 5 displays the excitation energies of the $I^\pi = 3^-$ and 4^- states resulting from the $K^\pi = 0^-$ and 1^- octupole sequences, respectively, in the $N = 90$ nuclei. For ^{156}Dy, we have associated bands 2 and 4 with these two sequences, respectively. Note that the 3^- and 4^- states are much closer to each other in gadolinium ($Z = 64$) and dysprosium ($Z = 66$) than in samarium ($Z = 62$), indicating that the $K^\pi = 0^-$ and 1^- sequences are relatively near each other in the former nuclei. This proximity could produce mixing between the $K^\pi = 0^-$ band and the odd-spin sequence of the $K^\pi = 1^-$ structure. In fact, there is evidence of this mixing as "normal" ordering of the $K^\pi = 1^-$ states is observed in ^{152}Sm (where the 1^- level is lowest in energy, followed successively by the 2^-, 3^-, 4^-... levels), but the odd-spin sequence is pushed up in energy (with respect to the even-spin structure) in ^{154}Gd (where the 2^- level is lowest in energy, followed by 1^-, 4^-, and 3^-). Therefore, if band 4 in ^{156}Dy is associated with the $K^\pi = 1^-$ octupole structure, one might expect its odd-spin partner to be shifted higher in energy due to mixing with band 2.

A candidate for a partner that validates this scenario is band 3, which is found at higher spin, as seen in Fig. 1. Figure 4(b) displays the alignments of bands 2, 3, 4, and 4a. Note that bands 3, 4, and 4a have approximately the same alignment profile and undergo a crossing at a similar frequency [that differs from the two-quasiparticle bands shown in Fig. 4(a)]. This similarity is suggestive of band 3 being a partner with bands 4 and 4a. A large energy splitting is observed between bands 3 and 4, which can be explained by the aforementioned mixing between bands 2 and 3.

Therefore, bands 2 and 4 are not likely partner bands as they differ in K, which can lead to differing $B(E2)/B(E1)$ ratios, as noted by Konijn *et al.* [23]. In fact, Löbner [26] discussed this difference four decades ago where it was found that "...there are more components in the wave functions of the octupole vibrational states with $K^\pi = 0^-$ which give rise to unhindered $E1$ transitions ... than for the $K^\pi = 1^-$ octupole vibrational levels." Thus, the difference in $B(E2)/B(E1)$ ratios between bands 2 and 4 does not necessarily indicate that the even-spin, negative-parity band is associated with tetrahedral symmetry. It should be noted that the $K^\pi = 2^-$ assignment cannot be completely ruled out as Neergärd and Vogel [20] suggested that the two may have similar excitation energies.

V. SUMMARY AND OUTLOOK

The negative-parity states in ^{156}Dy were investigated to examine whether the experimental signature for tetrahedral symmetry could be identified. A number of new or extended band structures were observed and three of the sequences can be readily understood as octupole vibrational bands: an odd-spin $K^\pi = 0^-$ sequence (band 2) and a possible $K^\pi = 1^-$ pair of bands (bands 3 and 4/4a). In addition, two new bands were identified that may be based on the energetically unfavored coupling of the $i_{13/2}$ and $f_{7/2}$ quasineutrons.

An early criterion for identifying structures associated with tetrahedral symmetry was a decrease of the $B(E2)$ strength between negative-parity rotational states towards zero as the sequence approaches the bandhead state. Measuring $B(E2)$ values directly in these bands is difficult, so the working criterion was to find bands where the $B(E2)/B(E1)$ ratios are small, indicative of a possible tetrahedral symmetry [2]. As shown in Table II, the $B(E2)/B(E1)$ ratio is indeed small for the odd-spin $K^\pi = 0^-$ sequence of states in ^{156}Dy. However, recent work on isotones of ^{156}Dy leads to the conclusion that the $B(E2)$ values in the equivalent bands in ^{154}Gd and ^{160}Yb are similar to those of the respective ground-state sequences [5, 6], and this is likely also the case for ^{156}Dy. The conclusion from the current experiment is that the observed negative-parity bands correspond to octupole excitations rather than to the exotic tetrahedral symmetry.

This conclusion is, perhaps, not surprising as the theory of this high-rank symmetry has evolved. Recent calculations [27] indicate that not only the quadrupole, but also the dipole transition moments should approach zero when the nuclear shape obeys tetrahedral symmetry. The result is that, even if the $B(E2)/B(E1)$ ra-

tio is finite, the $B(E2)$ and $B(E1)$ rates could both be close to zero; therefore, neither transition would be detectable and population of these states would be difficult. In addition, due to quadrupole oscillations in the tetrahedral minimum, it is possible that the quadrupole or dipole moments underlying these tetrahedral structures are very small up to relatively high spins. This would make population of such tetrahedral bands via enhanced $E1$ or $E2$ transitions almost impossible under the conditions of the present experiment. Instead, it is possible that tetrahedral states can only be populated via collective octupole ($E3$) transitions (in Coulomb excitation experiments) or through single-particle de-excitation from higher-lying bands in a compound-nuclear reaction that brings little angular momentum into the nucleus [27].

Ongoing theoretical work based on group representation theory and microscopic solutions of the many-body problem [28, 29] suggests that a near linear energy versus spin dependence should exist within tetrahedral bands. As none of the bands in ^{156}Dy meet this criterion, the existence of a tetrahedral minimum could not be confirmed from the present experiment. Such a sequence would make tetrahedral structures rather high lying (in the low-spin regime) compared to the usual rotational bands populated in heavy-ion reactions. A detailed theoretical analysis is in progress and will be published elsewhere [30].

In conclusion, the bands observed in ^{156}Dy via the present experiment exhibit no evidence for tetrahedral symmetry. Future experiments searching for these exotic structures should focus on other population mechanisms with the ability to look for more non-yrast excitations linked by weak $E1$ and $E2$ transitions to lower-lying states.

VI. ACKNOWLEDGMENTS

The authors thank the ANL operations staff at Gammasphere and gratefully acknowledge the efforts of J. P. Greene for target preparation. We thank D. C. Radford and H. Q. Jin for their software support. This work is funded by the National Science Foundation under Grant Nos. PHY-1203100 (USNA) and PHY-0754674 (FSU), as well as by the U.S. Department of Energy, Office of Science, Office of Nuclear Physics, under Contract Number DE-AC02-06CH11357 (ANL), and under award numbers DE-FG02-94ER40848 (UML), DE-FG02-96ER40983 (UT), DE-FG02-91ER40609 (Yale), DE-AC02-98CD10886 (BNL), and DE-FG02-94ER40834 (UM). J. S. would like to acknowledge the support of the UK Science and Technology Council (STFC). J. F. S-S. acknowledges support from the Joyce Frances Adlard Cultural Fund, and S. T. N. M. acknowledges the South African National Research Foundation. This research used resources of Argonne National Laboratory's ATLAS facility, which is a DOE Office of Science User Facility.

[1] J. Dudek, A. Góźdź, N. Schunck, and M. Miskiewicz, Phys. Rev. Lett. **88**, 252502 (2002).
[2] J. Dudek, D. Curien, N. Dubray, J. Dobaczewski, V. Pangon, P. Olbratowski, and N. Schunck, Phys. Rev. Lett. **97**, 072501 (2006).
[3] A. Dobrowolski, A. Góźdź, K. Mazurek, and J. Dudek, Int. J. Mod. Phys. E **20**, 500 (2011).
[4] J. Dudek, D. Curien, A. Góźdź, Y. R. Shimizu, and S. Tagami, Acta Phys. Pol. B **44**, 305 (2013).
[5] M. Jentschel, W. Urban, J. Krempel, D. Tonev, J. Dudek, D. Curien, B. Lauss, G. de Angelis, and P. Petkov, Phys. Rev. Lett. **104**, 222502 (2010).
[6] R. A. Bark *et al.*, Phys. Rev. Lett. **104**, 022501 (2010).
[7] M. Jentschel, L. Sengele, D. Curien, J. Dudek, and F. Haas, Phys. Scr. **89**, 054017 (2014).
[8] S. N. T. Majola *et al.*, Phys. Rev. C **91**, 034330 (2015).
[9] R. V. F. Janssens and F. S. Stephens, Nucl. Phys. News **6**, 9 (1996).
[10] M. Cromaz *et al.*, Nucl. Inst. Meth. A **462**, 519 (2001).
[11] D. C. Radford, Nucl. Inst. Meth. A **361**, 297 (1995).
[12] M. A. Riley *et al.*, Nucl. Phys. A **486**, 456 (1988).
[13] F. G. Kondev *et al.*, Phys. Lett. B **437**, 35 (1998).
[14] F. W. N. de Boer, P. Koldewijn, R. Beetz, J. L. Maarleveld, J. Konijn, R. V. F. Janssens, and J. Vervier, Nucl. Phys. A **290**, 173 (1977).
[15] M. A. Caprio *et al.*, Phys. Rev. C **66**, 054310 (2002).
[16] S. N. T. Majola, unpublished.
[17] F. G. Kondev, unpublished.
[18] C. W. Reich, Nucl. Data Sheets **113**, 2537 (2012).
[19] S. M. Harris, Phys. Rev. **138B**, 509 (1965).
[20] K. Neergård and P. Vogel, Nucl. Phys. **A145**, 33 (1970).
[21] P. A. Butler and W. Nazarewicz, Rev. Mod. Phys. **68**, 349 (1996).
[22] Krzysztof Zberecki, Paul-Henri Heenen, and Piotr Magierski, Phys. Rev. C **79**, 014319 (2009).
[23] Jan Konijn, F. W. N. de Boer, A. Van Poelgeest, W. H. A. Hesselink, M. J. A. de Voigt, H. Verheul, and O. Schölten, Nucl. Phys. **A352**, 191 (1981).
[24] P. E. Garrett *et al.*, Phys. Rev. Lett. **103**, 062501 (2009).
[25] C. W. Reich, Nucl. Data Sheets **110**, 2257 (2009).
[26] K. E. G. Löbner, "Gamma-ray Transition Probabilities in Deformed Nuclei," Chapter V of *The Electromagnetic Interaction in Nuclear Spectroscopy* (W. D. Hamilton, ed.) North-Holland Publishing Co., Amsterdam (1975).
[27] J. Dudek, D. Curien, D. Rouvel, K. Mazurek, Y. R. Shimizu, and S. Tagami, Phys. Scr. **89**, 054007 (2014).
[28] S. Tagami, Y. R. Shimizu, and J. Dudek, Phys. Rev. C **87**, 054306 (2013).
[29] S. Tagami, Y. R. Shimizu, and J. Dudek, J. Phys. G **42**, 015106 (2015).
[30] J. Dudek, priv. comm.